Inferring the genetic relationship between brain imaging-derived phenotypes and risk of complex diseases by Mendelian randomization and genome-wide colocalization

Siying Lin [a,b], Haoyang Zhang [b], Mengling Qi [a], David N. Cooper [c], Yuedong Yang [b,**], Yuanhao Yang [d,***], Huiying Zhao [a,*]

[a] Department of Medical Research Center, Sun Yat-Sen Memorial Hospital, Sun Yat-Sen University, Guangzhou 510120, China
[b] School of Computer Science and Engineering, Sun Yat-Sen University, Guangzhou 510006, China
[c] Institute of Medical Genetics, School of Medicine, Cardiff University, Heath Park, Cardiff CF14 4XN, United Kingdom
[d] Mater Research Institute, The University of Queensland, Brisbane, QLD, Australia

ARTICLE INFO

ABSTRACT

Observational studies consistently disclose brain imaging-derived phenotypes (IDPs) as critical markers for early diagnosis of both brain disorders and cardiovascular diseases. However, it remains unclear about the shared genetic landscape between brain IDPs and the risk of brain disorders and cardiovascular diseases, restricting the applications of potential diagnostic techniques through brain IDPs. Here, we reported genetic correlations and putative causal relationships between 921 brain IDPs, 20 brain disorders and six cardiovascular diseases by leveraging their large-scale genome-wide association study (GWAS) summary statistics. Applications of Mendelian randomization (MR) identified significant putative causal effects of multiple region-specific brain IDPs in relation to the increased risks for amyotrophic lateral sclerosis (ALS), major depressive disorder (MDD), autism spectrum disorder (ASD) and schizophrenia (SCZ). We also found brain IDPs specifically from temporal lobe as a putatively causal consequence of hypertension. The genome-wide colocalization analysis identified three genomic regions in which MDD, ASD and SCZ colocalized with the brain IDPs, and two novel SNPs to be associated with ASD, SCZ, and multiple brain IDPs. Furthermore, we identified a list of candidate genes involved in the shared genetics underlying pairs of brain IDPs and MDD, ASD, SCZ, ALS and hypertension. Our results provide novel insights into the genetic relationships between brain disorders and cardiovascular diseases and brain IDP, which may server as clues for using brain IDPs to predict risks of diseases.

1. Introduction

Brain imaging-derived phenotypes (IDPs) are measured non-invasively using magnetic resonance imaging (MRI) (Miller et al., 2016), and can potentiate the early diagnosis of brain disorders (Gong et al., 2021) and cardiovascular disease (McCracken et al., 2022). A previous study has found that adults with autism spectrum disorder (ASD) showed thicker frontal cortices compared with adult control subjects (Boedhoe et al., 2020). Fractional anisotropy (FA) has been found to be significantly lower in the corpus callosum and posterior

thalamic radiation regions of the brain in BID patients than among controls (Sarıçiçek et al., 2016). Interestingly, microstructural alterations in the brain have been found to be associated with cardiovascular disease (Sarıçiçek et al., 2016) whilst white matter hyperintensities have been found to be associated with the progression of hypertension (Hajjar et al., 2011). In addition, sleep traits have been linked to brain size (Vreeker et al., 2021) whilst insomnia has been associated with the right angular gyrus (Wei et al., 2019). Taken together, these studies have provided a considerable body of evidence to support the contention that IDPs are phenotypically associated with the risk of psychiatric, neurological, cardiovascular and sleep traits. However, the precise nature of the genetic relationships between IDPs and these disorders is still far from clear.

A number of genetic studies have been performed to identify variants associated with IDPs. Elliott et al. employed a genome-wide association study (GWAS) to reveal genetic variants associated with three MRI markers of brain disorders (Elliott et al., 2018). More recently, Smith et al. presented an open resource of GWAS summary statistics of 3144 brain IDPs (Smith et al., 2021). Using these large-scale GWAS summaries of brain IDPs, researchers have made strenuous efforts to develop methods for detecting brain features associated with both behavioral and neuropsychiatric traits (Liang et al., 2022). Meanwhile, the growing number of published GWAS over the past two decades has stimulated the emergence of an increasing number of methods for detecting cross-trait shared genetic architecture based on GWAS summary statistics. Thus, the linkage disequilibrium score (LDSC) statistic was presented by Bulik-Sullivan et al. as a means to estimate single nucleotide polymorphism (SNP)-based genetic correlations between traits (Bulik-Sullivan et al., 2015a). Mendelian randomization (MR) has been proposed as a means to measure the putatively causal relationship between traits. The basic concept of MR is to use genetic variants as instruments to mimic a random allocation procedure in randomized controlled trials, thereby avoiding issues of confounding and reverse causation (Emdin et al., 2017). The approach to identify the shared genetic etiology across multiple traits is colocalization analysis, such as HyPrColoc (Foley et al., 2021) and COLOC (Giambartolomei et al., 2014a). The purpose of colocalization analysis between traits is to identify variants associated with multiple traits (Foley et al., 2021). These variants may be causal according to the hypothesis of the colocalization analysis (Giambartolomei et al., 2018).

By using these approaches and datasets, researchers have achieved considerable success in terms of increasing our understanding of the shared genetic architecture between traits (Giambartolomei et al., 2014a; Giambartolomei et al., 2018; May-Wilson et al., 2022), in so doing providing us with novel biomarkers with which to assess disease risk or to design new therapeutic approaches. A recent study revealed genetic correlations between food preferences and brain IDPs by using GWAS summary statistics of 2329 IDPs [including brain functional MRI (fMRI)-related IDPs] (May-Wilson et al., 2022). Another study (Guo et al., 2022) used GWAS summary data to identify putatively causal relationships between 587 IDPs (excluding brain fMRI-related IDPs) and psychiatric disorders. Zhao et al. (2021) discovered many common variants associated with white matter features as well as neuropsychiatric disorders. Efforts have also been made to identify the genetic relationship between IDPs and Alzheimer disease (Knutson and Pan, 2020). However, as yet, no studies have been performed to identify the causal relationships between IDPs and neurological, psychiatric, and sleep traits and cardiovascular diseases, or the shared etiologies between them and IDPs.

In this study, we leveraged large-scale GWAS summary statistics and applied linkage disequilibrium score regression (LDSC) to estimate the genetic correlation between 921 IDPs and 26 disorders, including 8 psychiatric disorders, 6 neurological disorders, 6 cardiovascular diseases and 6 sleep traits. The genetic relationships between the brain IDPs and these disorders were detected by MR and colocalization analysis. Additionally, we identified pleiotropic genes associated with the

disorders and brain IDPs by gene-based genome-wide association study and pleiotropy testing. This study provides evidence for causal relationships between eight IDPs and the risks of four psychiatric disorders and one cardiovascular disease. These IDPs represent potentially novel biomarkers for the early-stage diagnosis, prevention and monitoring of these disorders. Further, this study offers new insights into the shared genetic mechanisms underlying the relationship between the IDPs and the diseases through pleiotropic gene analysis. A schematic overview of the design of this study is depicted in Fig. 1.

2. Methods

2.1. Overview of the study

Fig. 1 depicts the overall design of this study. The study itself comprises five modules. (1) We collected GWAS summary statistics of 921 brain IDPs (Smith et al., 2021), and the GWAS summary statistics of 8 psychiatric disorders, 6 neurological disorders, 6 cardiovascular diseases and 6 sleep traits from the Psychiatric Genomics Consortium (PGC) and NHGRI-EBI GWAS Catalog data (MacArthur et al., 2017). (2) We analyzed the genetic correlations between the IDPs and these disorders/diseases ($r_{gIDP\text{-}dis}$) by LDSC. (3) We investigated whether the genetic correlations ($r_{gIDP\text{-}dis}$) between them were sufficient to account for the genetic correlations ($r_{g\text{-}dis\text{-}dis}$) between the disorders. (4) We evaluated the putative causal relationships between the brain IDPs and the disorders by MR analysis. We further used colocalization analysis to identify the causal SNPs associated with brain IDPs and the disorders. (5) To identify the shared genetic mechanisms of the disorders and IDPs, we performed gene-level genome-wide association analysis. Below are the details describing the methods used in each module.

2.2. Data resources

GWAS summary statistics for 26 brain disorders and cardiovascular diseases were collected from the Psychiatric Genomics Consortium (PGC) and NHGRI-EBI GWAS Catalog data (MacArthur et al., 2017) (Supplementary Table 1), with sample sizes ranging from 10,240 to 977, 323. These disorders included 8 psychiatric disorders (major depressive disorder, bipolar disorder, autism spectrum disorder, schizophrenia, attention deficit hyperactivity disorder, post-traumatic stress disorder, panic disorder and anorexia nervosa), 6 neurological disorders (stroke, Parkinson disease, Alzheimer disease, multiple sclerosis, amyotrophic lateral sclerosis and epilepsy), 6 cardiovascular diseases (coronary atherosclerosis, angina pectoris, hypertension, myocardial infarction, cardiac hypertrophy and heart failure) and 6 sleep traits (insomnia, narcolepsy, sleep apnea, waking too early, sleeping too much and trouble falling asleep). We selected these disorders and diseases because they are common in the population and have available GWAS summary data based on large sample size (>100,00).

A total of 921 publicly available GWAS summary statistics of brain IDPs (Supplementary Table 2), generated from 33,224 individuals, were also downloaded from the Oxford Brain Imaging Genetics Server-BIG40 (https://open.win.ox.ac.uk/ukbiobank/big40/) (Smith et al., 2021). The GWAS summary statistics of these 921 IDPs included 776 structural MRI features and 145 diffusion MRI features. These MRI measures covered the cerebral cortex, subcortical regions and white matter tracts. All GWAS summary statistics were European-based and processed after excluding non-biallelic SNPs, SNPs with strand-ambiguous alleles, duplicated SNPs, SNPs that were not identified by the 1000 Genomes Project European reference, SNPs located in the major histocompatibility complex (MHC) region (chromosome 6: 28.5–33.5 Mb) and SNPs with a minor allele frequency (MAF) < 0.01. In this study, we only considered structural MRI and diffusion MRI-related IDP, while most IDPs are resting-state functional MRI-related ($n>1700$). The reason why we did not include resting-state functional MRI-related IDPs is that they usually involve multiple brain regions and their genetic correlations to
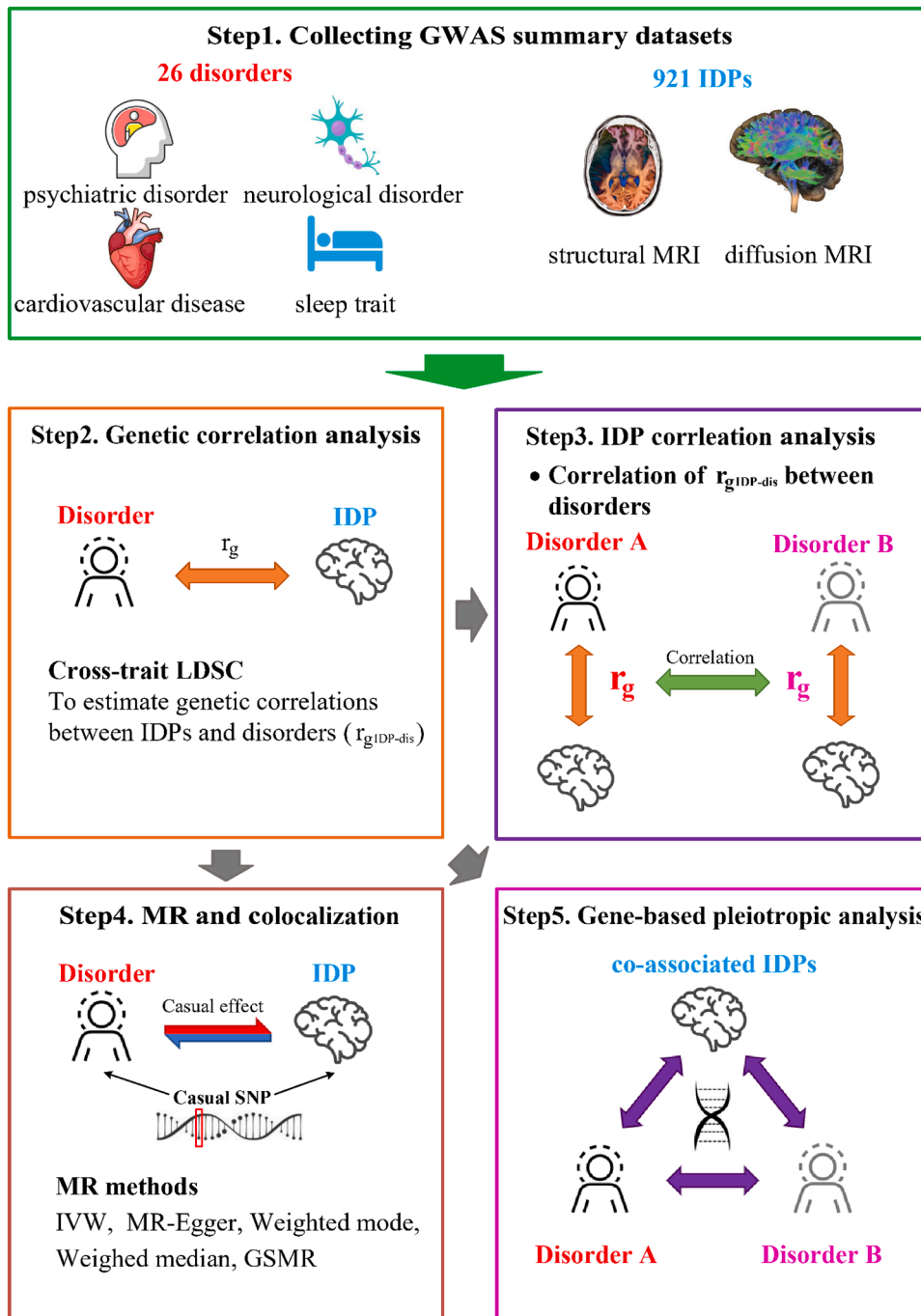
Fig. 1. Schematics for the genetic analysis of relationships between IDPs and brain disorders. **Step 1.** GWAS summary statistics of 921 IDPs include 776 structural magnetic resonance imaging (MRI) features and 145 diffusion MRI features distributed in cerebral cortex, subcortical regions and white matter tracts, and the GWAS summary statistics of diseases include 8 psychiatric disorders, 6 neurological disorders, 6 cardiovascular diseases and 6 sleep traits, which were downloaded from the Psychiatric Genomics Consortium (PGC) or the NHGRI-EBI GWAS Catalog. **Step 2.** Analysis of genetic correlations between the IDPs and the brain disorders/cardiovascular diseases ($r_{gIDP\text{-}dis}$) by LDSC. **Step 3.** To investigate whether the genetic correlations between the disorders and IDPs were able to account for the genetic correlations between disorders, the Pearson correlation coefficient (PCC) was calculated between the $r_{gIDP\text{-}dis}$ of all pairs of disorders. **Step 4.** We evaluated the putative causal relationships between the brain IDPs and the disorders by Mendelian Randomization (MR) analysis. We further used colocalization analysis to identify the causal SNPs associated with brain IDPs and the disorders. Step 5. To identify the shared genetic mechanisms between the disorders and IDPs, we performed gene-level genome-wide association analysis by MAGMA, and a gene-level pleiotropic test by PLACO.

disorder is relatively complex.

2.3. Linkage disequilibrium score regression

LDSC is used to estimate genetic correlations between traits based on GWAS summary statistics (Bulik-Sullivan et al., 2015b). The genetic correlations between the disorders and the IDPs were estimated by cross-trait LDSC. The European-ancestry population of 1000 Genomes Project Phase 3 was used as the reference panel for the analysis (Bulik-Sullivan et al., 2015a). Then, LDSC was performed, under a weighted linear model, by regressing the product of Z-statistics of two traits with the LD scores of the genome-wide SNPs. The significant genetic correlations were determined with $P < 0.05$.

2.4. Estimating genetic correlations between the brain disorders and cardiovascular diseases according to their correlations with brain IDPs

The cross-trait LDSC was firstly used to estimate the genetic correlations between the brain disorders/cardiovascular diseases and the IDPs ($r_{gIDP\text{-}dis}$), as well as the genetic correlations between the brain disorders and the cardiovascular diseases ($r_{g\text{-}dis\text{-}dis}$). Then, we wonder whether the genetic correlations between the brain disorders and the cardiovascular diseases could be explained proportionally by their correlations with brain IDPs. We estimated the Pearson correlation coefficients (PCC) of $r_{gIDP\text{-}dis}$ for each pair of disorders/diseases, termed $PCC_{dis\text{-}IDP\text{-}dis}$ for the brain IDPs with significant genetic correlations with disorders ($P\ r_{gIDP\text{-}dis} < 0.05$).

Then, we employed the random skewers method in the R packges

"phytools" and 'unifcorrmat' (Revell, 2012) to estimate the similarity between $PCC_{dis\text{-}IDP\text{-}dis}$ matrix and $r_{g\text{-}dis\text{-}dis}$ matrix. The random skewed method has been widely used to estimate the similarity between two matrices (Cheverud, 1996). It calculates the vector correlation between the response vectors produced from the same set of random selection vectors applied to each matrix, using the Lande equation. Specifically, this method involves multiplying a matrix by many random vectors drawn from a uniform distribution over all possible vector directions and then measure the vector correlation between the response. The comparisons are usually made using the average angle (or cosine) of the response vectors to an a priori vector or to the response vectors corresponding from another matrix.

2.5. Mendelian randomization (MR) analysis

Multiple MR models were applied to investigate the putative causal relationships between brain IDPs and brain disorders/cardiovascular diseases with a nominally significant genetic correlation. MR evaluates the causal effect of a risk factor (i.e., exposure) on a target trait (i.e., outcome) using exposure-associated genome-wide significant genetic variants as instruments, assuming that the instrumental genetic variants have causal effects on the outcome only through the exposure. However, causal relationship may be confounded by the presence of horizontal pleiotropy, referring to the situation that instrumental SNPs affect the outcome via a non-causal pathway. To distinguish causality from horizontal pleiotropy, multiple MR models were applied, which are based on different assumptions on horizontal pleiotropy, including inverse variance-weighted (IVW), MR-Egger, weighted mode, weighed median, and generalized summary data-based Mendelian randomization (GSMR). IVW integrates the GWAS effect ratios of instrumental SNPs and uses a weighted linear regression to calculate the causal estimate without correcting horizontal pleiotropy (Burgess et al., 2016). MR-Egger is a simple modification of IVW through the addition of an intercept term that captures the non-zero (weighted) average pleiotropic effect (Bowden et al., 2015). The weighted mode model calculates the causal effect from the most frequent instrumental SNPs, which loosens the assumption of the weighted median model (i.e., pleiotropy occurs in less than half of instrumental SNPs) (Hartwig et al., 2017). The weighted median model measures the causal effect using the weighted median of the SNP ratio to reduce the impact from pleiotropic SNPs (Bowden et al., 2016). GSMR assumes the presence of uncorrelated pleiotropy and excludes such effects by outlier removal using the heterogeneity inherent in the dependent instrument (HEIDI) approach (Zhu et al., 2018). The MR analyses were performed by R packages "TwoSampleMR" (version 0.5.5) and "GSMR" (version 1.0.9). For these five MR methods, we selected instrumental SNPs with GWAS $P < 5 \times 10^{-8}$, and clumped with LD $r^2 < 0.05$ within a 1Mb window using PLINK 1.9 (Purcell et al., 2007) according to the same 1000 Genomes Project reference described above (Bulik-Sullivan et al., 2015a). In order to ensure that there are no common causes of the genetic variant(s) and the outcome of interest, we removed SNPs associated with confounders that interfere with the pathway between brain structures and psychiatric disorders. We considered four potential confounders, including education, drinking and smoking behavior. These traits have been reported by previous studies to influence both psychiatric disorders (Gurillo et al., 2015; Schneider et al., 2014) and alterations of brain structure (Noble et al., 2015; Li et al., 2021). We obtained 2273 exposure-outcome pairs with the number of instrumental SNPs (SNPs robustly associated with the risk factor/exposure of interest) larger than 5. A significant causal relationship was determined if the P-value surpassed the Bonferroni-corrected significance level (i.e., $P < 0.05/2273 = \sim 2.20 \times 10^{-5}$). We also conducted MR-PRESSO (Mendelian randomization pleiotropy residual sum and outlier) test (Verbanck et al., 2018) to detect whether there was an independent pathway between the genetic variants and the outcome other than through the exposure. P-value larger than 0.05 was regarded as no horizontal pleiotropy in the statistical significance test.

2.6. Colocalization analysis

Colocalization analysis was performed to assess whether the brain disorders/cardiovascular diseases and brain IDP share common genetic causal variants in a genomic region. We implemented colocalization analysis by using COLOC (Giambartolomei et al., 2014b) to detect shared causal SNPs between the two traits. COLOC assumes at most one association per trait in a test region and uses Approximate Bayes Factor computation to generate posterior probabilities (PP) of all possible configurations between two traits: 1) H0: no association with either trait; 2) H1: association with trait 1, not with trait 2; 3) H2: association with trait 2, not with trait 1; 4) H3: association with trait 1 and trait 2, two distinct SNPs; 5) H4: association with trait 1 and trait 2, one shared SNP. The PP of each configuration is respectively denoted by PP_0, PP_1, PP_2, PP_3, and PP_4. A large PP_4 (e.g., $PP_4 > 90\%$) was considered to be strong support for colocalization in the original method publication (Giambartolomei et al., 2014b), which indicated a shared variant between disorder and brain IDP. Genomic regions were defined within 100 kb of the instrumental SNP variables. We set the prior probability of each SNP that is causal to either of the traits to 1×10^{-4} (i.e. one in 10, 000 SNPs in the genome are causal to either trait) and causal to both traits to 1×10^{-6} (i.e. one in 100 SNPs in the genome causal to one trait are causal to both traits). SNPs with the maximum PP4 are most likely to be causal to both two traits, and are thus selected as the candidate causal SNPs.

2.7. Gene-based association analysis and pleiotropic analysis

Next, Multi-marker Analysis of GenoMic Annotation (MAGMA) (de Leeuw et al., 2015) was applied to detect candidate genes associated with specific pairs of brain IDPs and brain disorders/cardiovascular diseases. MAGMA converts GWAS-based SNP-level associations into gene-level associations using a multiple regression method to incorporate linkage disequilibrium (LD) between variants and to discover multi-variant effects. The 1000 Genomes Project European-based LD reference panels were utilized to correct LD structure. We defined the set of SNPs as those located within a given gene according to the annotation file provided by https://ctg.cncr.nl/software/magma. For each gene, MAGMA provided a P value to evaluate its association with the disorder. If $FDR_{MAGMA} < 0.05$ in MAGMA test, the gene was considered to be significantly associated with the trait.

The P value provided by the MAGMA analysis was converted into Z statistics. Employing these transformed Z statistics, we applied a method called Pleiotropic Analysis under Composite Null Hypothesis (PLACO) (Ray and Chatterjee, 2020) to carry out the pleiotropy analysis. PLACO is used to identify pleiotropic loci between two traits by testing the composite null hypothesis that a locus is associated with zero or one of the traits. We extended it here in order to discover pleiotropic associations between traits at the gene level. PLACO examines the associations of one gene with two traits according to Z-statistics and divides the composite null hypothesis of pleiotropy into three null sub-hypotheses: the gene is associated with the first disorder but not the second; the gene is associated with the second disorder but not the first; and the gene is not associated with either of the two disorders. The alternative hypothesis is that the gene is associated with both disorders, corresponding to a pleiotropic association. The P values of MAGMA and PLACO were corrected by false discovery rate (FDR). If $FDR_{PLACO} < 0.05$, the gene was considered to be a pleiotropic gene associated with two traits. For the IDP that is genetically co-associated with two traits, A and B, we obtained two sets of pleiotropic genes, A-IDP and B-IDP by conducting PLACO. Then, we applied hypergeometric distribution to check the significance of the overlap of the two pleiotropic gene sets. The significance is based on the Bonferroni-corrected P (i.e., less than 0.05/53 disorder-disorder pairs with pleiotropic gene overlap $\approx 9.43 \times 10^{-4}$).

3. Results

3.1. Genetic correlations between brain IDPs and brain disorders/cardiovascular diseases

We used cross-trait LDSC to estimate the genetic correlation between 921 brain IDPs and 26 brain disorders/cardiovascular diseases. A total of 2171 pairs of brain IDPs and brain disorders/cardiovascular diseases were estimated with a nominally significant r_g ($P<0.05$), ranging from -0.75 to 0.83 (Supplementary Table 3 and Supplementary Figure 1A). Fig. 2A shows the numbers of IDPs genetically correlated ($P<0.05$) with the disorders, where narcolepsy (NAR) was genetically correlated

Fig. 2. The genetic correlations between IDPs and various disorders/diseases. **A.** The numbers of IDPs genetically correlated ($P<0.05$) with 26 disorders. **B.** The brain region distribution of IDPs that are genetically correlated with the psychiatric disorders, neurological disorders, cardiovascular diseases and sleep traits. "*" indicates Binomial test $P<0.05/72$ [72 is the number of tests (4 disorder categories × 18 brain regions)].

($P<0.05$) with 204 IDPs, followed by anorexia nervosa (AN, 160 IDPs), major depressive disorder (MDD, 150 IDPs) and stroke (STR, 145 IDPs). The genetic correlations between the brain disorders/cardiovascular diseases and the IDPs in 18 brain regions are shown in Supplementary Figure 1B-F. Among them, four pairs of brain IDPs and disorders surpassed the Bonferroni significance level ($P < 0.05/921 = ~5.43 \times 10^{-5}$): mean fractional anisotropy (FA) in posterior right corona radiata and narcolepsy ($r_g = 0.54$; $P = 1.23 \times 10^{-5}$), mean intra-cellular volume fraction (ICVF) in posterior left thalamic radiation and narcolepsy ($r_g = 0.51$; $P = 3.77 \times 10^{-5}$), mean isotropic or free water volume fraction (ISOVF) in superior left longitudinal fasciculus and stroke ($r_g = -0.46$; $P = 2.27 \times 10^{-5}$), and mean ICVF in genu of corpus callosum and major depressive disorder ($r_g = 0.15$; $P = 4.34 \times 10^{-5}$).

We also found that psychiatric disorders were more likely to genetically correlate with brain IDPs from the whole brain (Binomial test $P = 1.92 \times 10^{-6}$), corona radiata (Binomial test $P = 1.76 \times 10^{-4}$) and corpus callosum (Binomial test $P = 2.31 \times 10^{-4}$), compared to other regions (Fig. 2B). In similar vein, cardiovascular diseases were more likely to genetically correlate with the brain IDPs from corona radiata (Binomial test $P = 3.58 \times 10^{-11}$), capsule (Binomial test $P = 7.16 \times 10^{-7}$) and whole brain (Binomial test $P = 1.42 \times 10^{-4}$), compared to other regions.

3.2. Genetic correlations between the brain disorders and cardiovascular diseases explained by their correlations with brain IDPs

Next, we explored whether the genetic correlations between the brain disorders and cardiovascular diseases could be explained proportionally by their correlations with brain IDPs. The absolute value of r_g ($P_{rg} < 0.05$) between brain IDPs and the disorders are ranged from 0.077 to 0.832 (Supplementary Figure 1C). We examined the skewness of the r_g distribution for each disorder by Kolmogorov-Smirnov Test, and found r_g distribution does not have significant skewness ($P>0.05$). Thus, it is
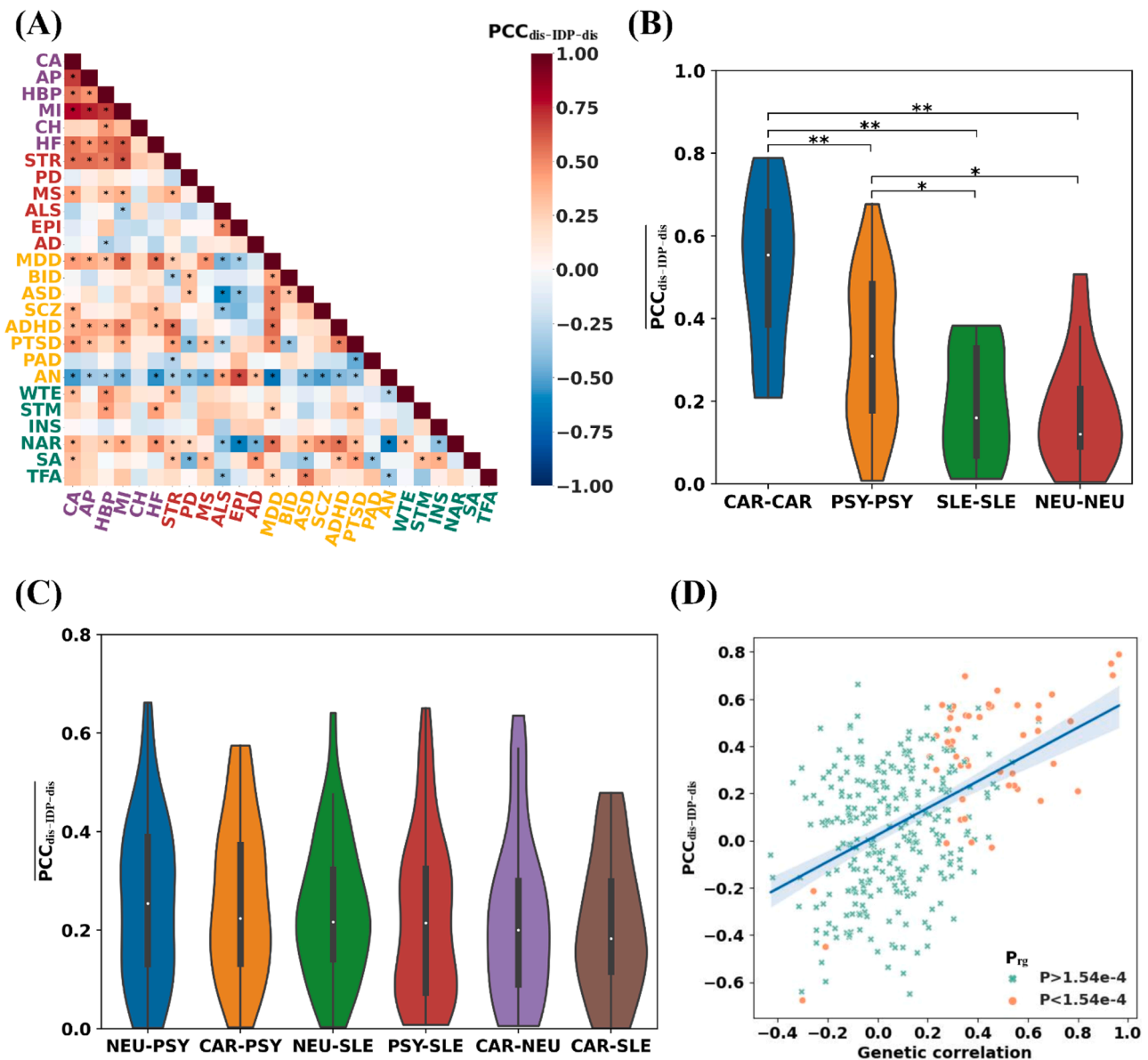
Fig. 3. Genetic correlations between disorders/diseases explained by the genetic correlations between the disorders/diseases and IDPs. **A.** The Pearson correlation coefficients ($PCC_{dis-IDP-dis}$) of the $r_{gIDP-dis}$ (genetic correlations between IDPs and disorders) across disorders. "*" indicates $P_{pcc} < 0.05/ (13\times25)$. **B.** Distribution of $PCC_{dis-IDP-dis}$ for the disorders from the same categories. **C.** Distribution of $PCC_{dis-IDP-dis}$ for the disorders from the different disorder categories. "*" indicates $0.001<t$-test $P<0.05$; "**" indicates t-test $P<0.001$. **D.** The Pearson correlation coefficients of $PCC_{dis-IDP-dis}$ and $r_{g-dis-dis}$ (genetic correlations between disorders). X-axis: $r_{g-dis-dis}$; Y-axis: $PCC_{dis-IDP-dis}$. PSY: psychiatric disorder; CAR: cardiovascular disease; NEU: neurological disorder; SLE: sleep trait.

reasonable to use PCC in estimating the correlations between $r_{gIDP\text{-}dis}$. We estimated the Pearson correlation coefficients (PCC) of $r_{gIDP\text{-}dis}$ for each pair of disorders/diseases, termed $PCC_{dis\text{-}IDP\text{-}dis}$ (Supplementary Table 4). Here, $r_{gIDP\text{-}dis}$ is the genetic correlation between one IDP and one disorder/disease, which is estimated by LDSC. As shown in Fig. 3A, we identified 81 (81/118, 68.6%) pairs that exhibited a positive correlation ($PCC_{dis\text{-}IDP\text{-}dis} > 0$ and $P_{pcc} < 0.05/325 = \sim1.54 \times 10^{-4}$) with an average of $PCC_{dis\text{-}IDP\text{-}dis}$ of 0.28, and 37 pairs that displayed a negative correlation ($PCC_{dis\text{-}IDP\text{-}dis} < 0$ and $P_{pcc} < 0.05/325 = \sim1.54 \times 10^{-4}$). When we compared the $PCC_{dis\text{-}IDP\text{-}dis}$ values that were estimated based on the disorders/diseases from the same disorder/disease category (Fig. 3B), we observed that the $PCC_{dis\text{-}IDP\text{-}dis}$ values of the cardiovascular diseases (average $PCC_{dis\text{-}IDP\text{-}dis} = 0.55$; t-test $P = 5.34 \times 10^{-8}$) and the psychiatric disorders (average $PCC_{dis\text{-}IDP\text{-}dis} = 0.31$; t-test $P = 2.30 \times 10^{-3}$) were significantly higher than the other two disorder categories (neurological disorders and sleep traits). Intriguingly, all the cardiovascular diseases exhibit positive correlations with $PCC_{dis\text{-}IDP\text{-}dis}$, ranging from 0.21 to 0.79. When we examined the $PCC_{dis\text{-}IDP\text{-}dis}$ values of disorders from different disorder categories (Fig. 3C), we found that the neurological and psychiatric disorders exhibited the highest average value (average $PCC_{dis\text{-}IDP\text{-}dis} = 0.25$) compared to others. We additionally used Spearman correlation (SPC) coefficient to estimate the correlations between $r_{gIDP\text{-}dis}$, and found 107 pairs that exhibited a significant correlation ($P_{spc} < 0.05/325 = \sim1.54 \times 10^{-4}$ and $P_{pcc} < 0.05/325 = \sim1.54 \times 10^{-4}$), consistent with the Pearson correlation result (Supplementary Table 4).

We further checked whether $PCC_{dis\text{-}IDP\text{-}dis}$ values significantly correlated with $r_{g\text{-}dis\text{-}dis}$ (genetic correlations between two disorders/diseases). Using the random skewers approach (Rohlf, 2017), we found that the $PCC_{dis\text{-}IDP\text{-}dis}$ matrix was significantly ($r = 0.73$, $P < 0.01$) correlated to the matrix of $r_{g\text{-}dis\text{-}dis}$. In addition, we estimated PCC between $PCC_{dis\text{-}IDP\text{-}dis}$ and $r_{g\text{-}dis\text{-}dis}$ of 51 genetically correlated ($P<0.05/325 = \sim1.54 \times 10^{-4}$) disorders/disease pairs, and found the PCC reached 0.63 ($P = 7.24 \times 10^{-7}$) (Fig. 3D), indicating that disorders/diseases sharing significant genetic associations tend to have similar genetic correlations with IDPs.

Considering that many IDPs are from the same brain regions using different imaging techniques, we examined if the r_g between IDPs from the same brain regions and disorders are highly correlated. Firstly, we examined if the r_g between IDPs from the same brain regions and disorders are highly correlated. The average of the absolute value of PCC is 0.60 (absolute value of PCC ranged from 0.43 to 0.95 and including 96 pairs with $P_{pcc} < 0.05/325 = \sim1.54 \times 10^{-4}$) significantly higher ($P_{t\text{-}test} = 1.27 \times 10^{-3}$) than the average of the absolute value of PCC 0.43 (absolute value of PCC ranged from 0.23 to 0.79 and including 118 pairs with $P_{pcc} < 0.05/325 = \sim1.54 \times 10^{-4}$) obtained using IDPs from the different brain regions. Thus, although the IDPs from the same brain regions have higher correlations (PCC) in r_g between IDPs and disorders, using the IDPs from the different brain regions to calculate PCC still shows consistent result with using IDPs from the same brain regions.

3.3. Putative causal relationships among brain IDPs, brain disorders and cardiovascular diseases

Afterwards, we applied multiple MR models to investigate whether the nominally significant r_g between specific pairs of brain IDPs and brain disorders/cardiovascular diseases could be explained by causality or horizontal pleiotropy. The quality control of the GWAS summary statistics yielded 2273 exposure-outcome pairs (including 1404 IDP-disorder pairs and 869 disorder-IDP pairs, considering two causal directions) with the number of instrumental SNPs larger than 5, including 1527 pairs with more than 10 instrumental SNPs. The results of MR analysis are shown in Supplementary Table 5–6. No horizontal pleiotropy was found by using the global test of MR-PRESSO (Supplementary Table 7).

We identified statistically significant ($P<0.05/2273 = \sim2.20 \times$ 10^{-5}) and putative causal effects of four IDPs in relation to the brain disorders. As shown in Fig. 4A, the mean orientation dispersion index (ODI) in right cerebral peduncle was identified as having a putatively causal effect on ALS (IVW OR = 0.80, 95% CI: 0.72 to 0.89, $P = 1.93 \times 10^{-5}$). We found that a per standard deviation (s.d.) decrease of the ODI in right cerebral peduncle was associated with a ~20% increase in ALS risk. A reduced ODI appears to imply a reduction in the complexity of dendrites and axons. This supports the notion that loss of motor neuron axon density is a core feature of the neurodegenerative process associated with ALS, consistent with previous pathological studies (Broad et al., 2019; Kamagata et al., 2021). Another IDP, the volume of lateral posterior (LP) nucleus of the thalamic nuclei in the left hemisphere, was found to have a putatively causal effect on MDD (IVW OR = 1.22, 95% CI of 1.11 to 1.35, $P = 1.93 \times 10^{-5}$), suggesting that a 1 s.d. increase of the volume of LP nucleus of the thalamic nuclei in the left hemisphere leads to a 22% increase in MDD risk (Fig. 4A). For ASD, we identified the mean intracellular volume fraction (ICVF) value of the superior fronto-occipital fasciculus in the right hemisphere as a putatively causal effect on ASD, suggesting that an increase of 1 s.d. in the ICVF value of the superior fronto-occipital fasciculus in the right hemisphere is associated with a 31% higher risk of ASD (IVW OR = 1.31, 95% CI of 1.17 to 1.46, $P = 1.49 \times 10^{-6}$). The fronto-occipital fasciculus is known to play a role in the control of neuropsychological behavior (D et al., 2021). Moreover, the increased ICVF appears to imply a reduction in the complexity of neurite density, which supports the notion that ASD is associated with the loss of motor neurite density (DiPiero et al., 2023). In addition, the volume of cerebellar white matter in the right hemisphere was found to have a putatively causal effect on increased SCZ risk with an estimated OR of 1.54 (95% CI 1.30–1.81, $P = 3.38 \times 10^{-7}$) (Fig. 4A). This is consistent with the observation that cerebellar white matter activity is a contributory factor to schizophrenia pathology (Yang et al., 2020; Papiol et al., 2014).

We also identified putative causal effects of hypertension (HBP) on four brain IDPs relate to the temporal lobe (superior, middle and inferior), with IVW P ranging from 1.11×10^{-6} to 2.18×10^{-5} (Fig. 4B). Temporal lobe is most commonly associated with processing auditory information and with the encoding of memory. Higher risk of hypertension was associated with decreased volume of the superior temporal lobe (IVW OR = 0.80, 95% CI of 0.73 to 0.89, $P = 1.39 \times 10^{-5}$), decreased thickness of the inferior temporal lobe (IVW OR = 0.79, 95% CI of 0.71 to 0.88, $P = 1.88 \times 10^{-5}$), decreased thickness of the middle temporal lobe (IVW OR = 0.81, 95% CI of 0.75 to 0.88, $P = 1.11 \times 10^{-6}$) and inferior temporal lobe (IVW OR = 0.80, 95% CI of 0.73 to 0.89, $P = 2.18 \times 10^{-5}$). Our result suggests that hypertension might be associated with reduced hippocampal connectivity and impaired memory. Fig. 4C summarizes the brain structure categories associated with the IDPs that exhibit putatively causal relationships with various disorders. The results of MR analysis which were based on fewer than 10 instrumental SNPs are shown in Supplementary Figure 4.

When we performed phenotypic association analysis (using logistic regression adjusted by age and sex) between four disorders (ASD, SCZ, MDD and ALS) and IDPs by using 37,224 samples from UK-biobank, we have not found the strong correlations (ASD: effect size = 1.37, $P = 3.93 \times 10^{-1}$; SCZ: effect size = 1.64, $P = 1.21 \times 10^{-2}$; MDD: effect size = 1.33, $P = 5.14 \times 10^{-2}$; ALS: effect size = 0.33, $P = 6.23 \times 10^{-2}$;). The underlying reason may due to the limited number of cases (12 ASD patients; 53 SCZ patients; 37 MDD patients; 25 ALS patients) in UK-Biobank. Further enlarging sample size is required in the to reveal the phenotypic correlations between ALS and ODI.

3.4. Colocalization analysis for brain IDPs, brain disorders and cardiovascular diseases

Although the MR analysis supports the casual relationships between brain IDPs and brain disorders/cardiovascular diseases, whether there are the genetic causal pathways shared between them is unknown. For
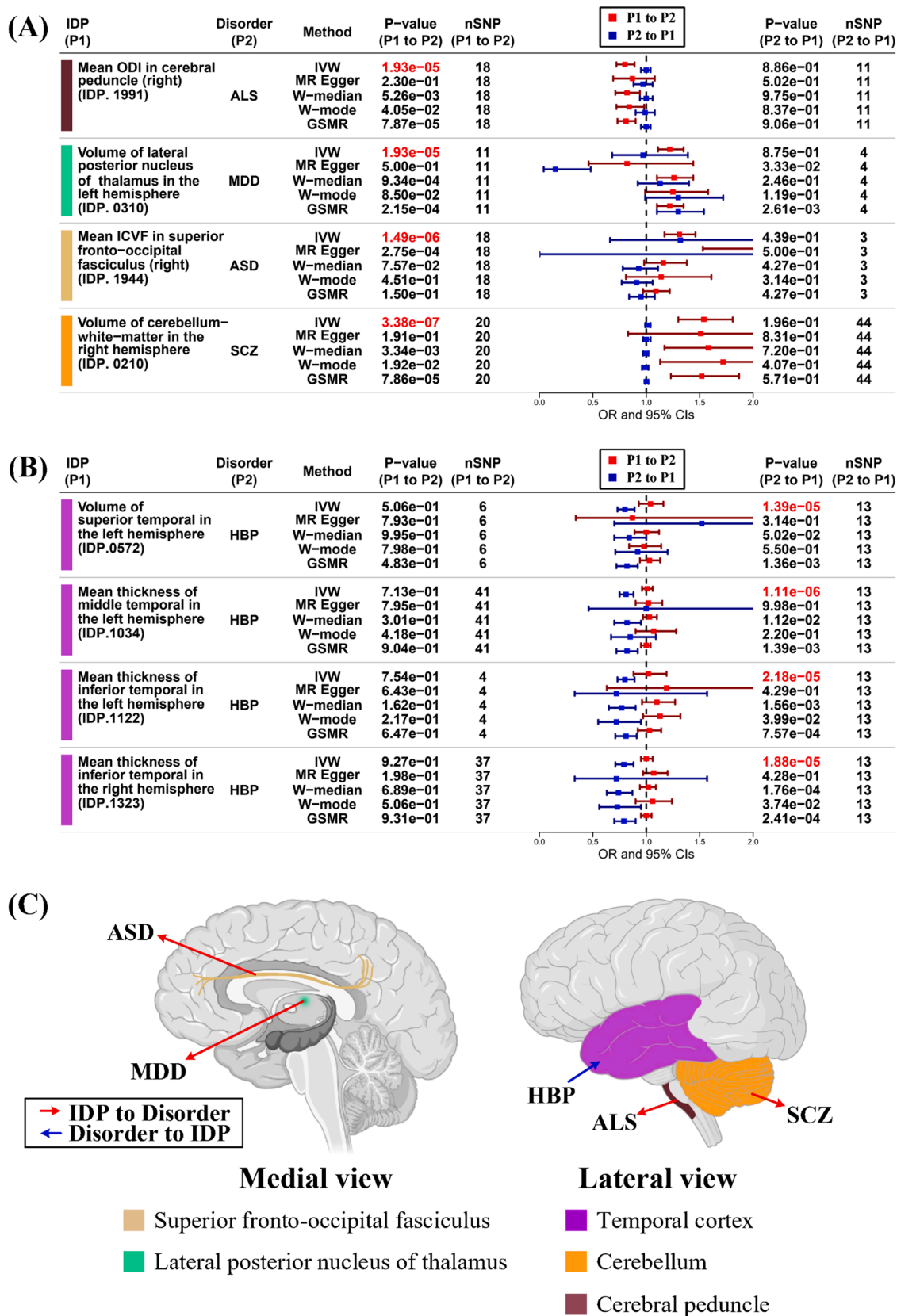
Fig. 4. Mendelian Randomization analysis to investigate the causal relationships between IDPs and various disorders/diseases. **A.** Forest plot showing the putative causal effects of IDPs on the disorders/diseases. **B.** Forest plot showing the putative causal effects of hypertension on the IDPs. **C.** Brain anatomical regions of the IDPs having putative causal relationships with ALS, MDD, ASD, SCZ and hypertension. ALS: amyotrophic lateral sclerosis; MDD: major depressive disorder; ASD: autism spectrum disorder; SCZ: schizophrenia; HBP: hypertension.

such purpose, we used COLOC to test shared causal SNPs between brain IDPs and brain disorders/cardiovascular diseases, which have shown putative causal relationships in MR analysis. The analysis indicated that MDD and volume of lateral posterior (LP) nucleus of the thalamic nuclei

in the left hemisphere are colocalized (PP$_4$ = 0.96) in one region of chromosome 7 (Fig. 5A), ASD and mean ICVF of the superior fronto-occipital fasciculus in the right hemisphere are colocalized (PP$_4$ = 0.95) in a region of chromosome 17 (Fig. 5B), and SCZ and volume of
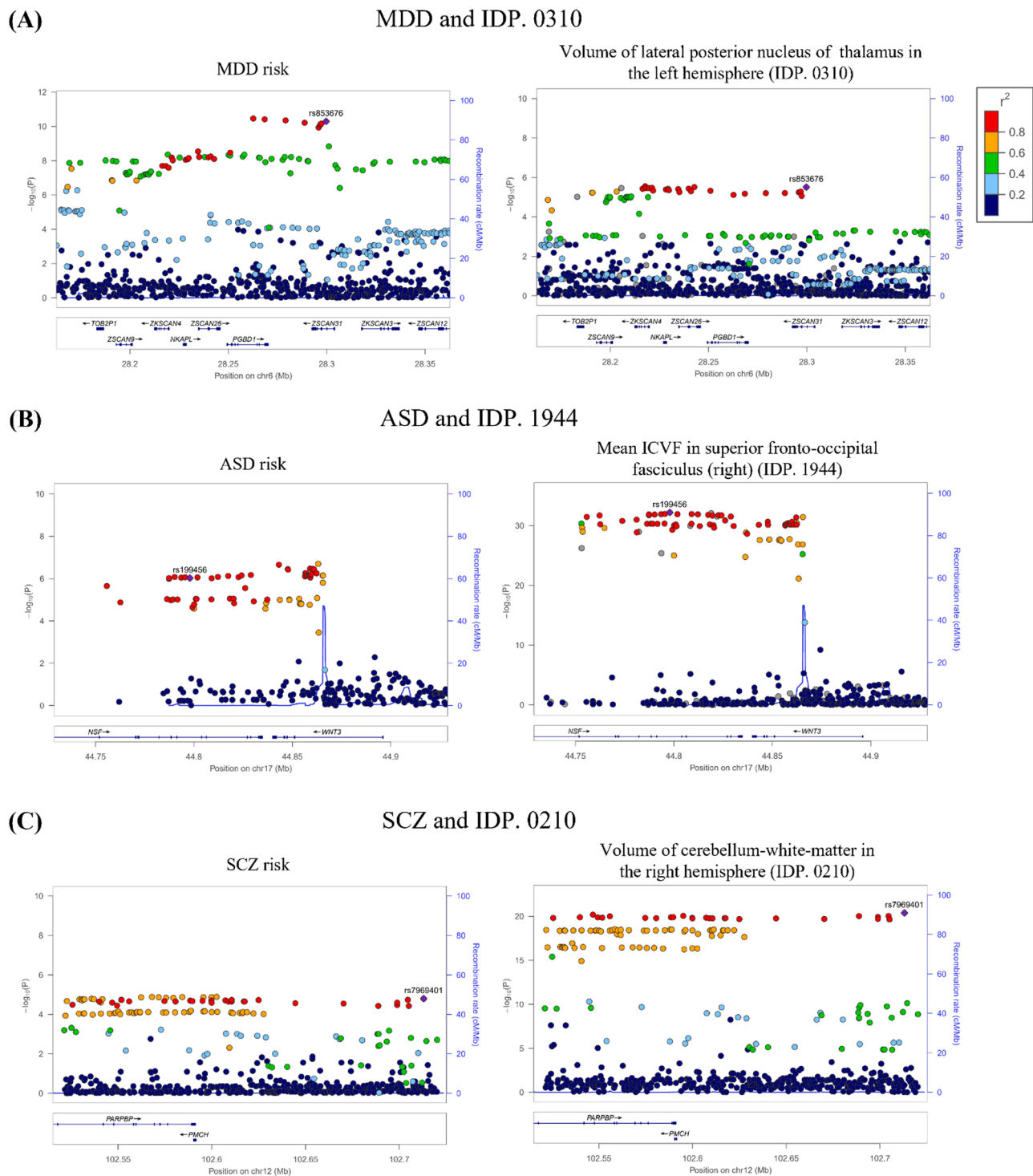

Fig. 5. Colocalization analysis depicting the genomic regions and causal SNPs associated with both the brain IDPs and various disorders/diseases. The x-axis shows position within the genome (building Hg19) and y-axis denotes the $-\log_{10}(P)$ for the association. Color denotes the LD between different variants. A. The colocalization analysis result for MDD and volume of lateral posterior nucleus of thalamus in the left hemisphere (IDP. 0310) indicated the SNP rs853676 ($P = 5.13 \times 10^{-11}$ GWAS for MDD and $P = 3.11 \times 10^{-6}$ GWAS for IDP. 0310) as a causal SNP associated with MDD and IDP. 0310. B. The colocalization analysis result for ASD and mean ICVF in superior fronto-occipital fasciculus (right) (IDP. 1944) indicated the SNP rs199456 ($P = 9.42 \times 10^{-7}$ GWAS for ASD and $P = 6.27 \times 10^{-33}$ GWAS for IDP. 1944) as a causal SNP associated with MDD and IDP. 0310. C. The colocalization analysis result for SCZ and volume of cerebellum-white-matter in the right hemisphere (IDP. 0210) indicated the SNP rs7969401 ($P = 1.59 \times 10^{-5}$ GWAS for SCZ and $P = 4.13 \times 10^{-21}$ GWAS for IDP. 0210) as a causal SNP associated with SCZ and IDP. 0210. MDD: major depressive disorder; ASD: autism spectrum disorder; SCZ: schizophrenia.

cerebellar white matter in the right hemisphere are colocalized (PP$_4$ = 0.90) in a region of chromosome 12 (Fig. 5C). The candidate causal SNPs in these three colocalized regions are rs853676, rs199456 and rs7969401 (Fig. 5A-C), respectively. Among these SNPs, rs199456 and rs7969401 have not been reported to be associated with ASD and SCZ, previously. The results of colocalization analysis are shown in Supplementary Table 8.

3.5. Candidate genes involved in the shared genetic mechanisms underlying brain IDPs and brain disorders/cardiovascular diseases

The MAGMA analysis was firstly performed on the brain IDPs and brain disorders/cardiovascular diseases that showed putative causal relationships. MAGMA analysis identified 20, 64, 150, 0 and 62 genes significantly ($FDR_{MAGMA} < 0.05$) associated with ALS, MDD, ASD, SCZ and HBP, respectively. MAGMA analysis also identified 250, 74, 87, 218, 17, 43, 84 and 3 genes significantly ($FDR_{MAGMA} < 0.05$) associated with eight IDPs (IDP.1991, IDP.0310, IDP.1944, IDP.0210, IDP.0572, IDP.1034, IDP.1122 and IDP.1223) (Table S2), which have putative causal effects on the disorders/diseases. The full name of each IDP was shown in Table S2. We further used Fisher's exact test to examine the significance of the number of shared genes between these disorders/diseases and the brain IDPs. The result indicated that the numbers of shared genes between the brain IDP, IDP.1944 (Table S2) and ASD (number of shared genes = 31, Fisher's exact test $P = 2.20 \times 10^{-43}$), and between the brain IDP, IDP.0310 and MDD (number of shared genes = 6, Fisher's exact test $P = 2.10 \times 10^{-7}$) are significantly more than the expected chance (Fig. 6A-B). The details of the shared genes are shown in Supplementary Table 9.

We further used PLACO to identify the pleiotropic genes associated with the brain IDPs and brain disorders/cardiovascular diseases that showed the putative causal relationships. We found that 1 pleiotropic gene ($FDR_{PLACO} < 0.05$) between ALS and mean ODI in right cerebral

peduncle, 36 pleiotropic genes ($FDR_{PLACO} < 0.05$) between MDD and volume of lateral posterior nucleus of the thalamic nuclei in the left hemisphere, 42 pleiotropic genes ($FDR_{PLACO} < 0.05$) between ASD and mean ICVF of the superior fronto-occipital fasciculus in the right hemisphere, and 1 pleiotropic gene ($FDR_{PLACO} < 0.05$) between SCZ and volume of cerebellar white matter in the right hemisphere (Supplementary Table 10). The PLACO analysis further indicated 34 pleiotropic genes between HBP and four IDPs relating to the temporal lobe (Supplementary Table 10). The pleiotropic genes discovered by PLACO (Bonferroni corrected $P < 0.05$) but not by MAGMA were shown in Fig. 6C. Notably, two genes (*PGBD1* and *ZKSCAN4*) that are near to the candidate causal SNP *rs853676* were identified to be the pleiotropic genes associated with MDD and the IDP, volume of lateral posterior nucleus of thalamus in the left hemisphere in both the MAGMA and PLACO analysis.

Totally, 95 candidate genes were identified as associated with the brain IDPs and 5 disorders (ALS, SCZ, MDD, ASD, and HBP) by PLACO analysis. To evaluate their enriched functions, we performed KEGG and gene ontology (GO) enrichment analyses by Metascape (Zhou et al., 2019) and KOBAS (Xie et al., 2011) web-based platform. By Metascape, the KEGG enrichment analysis shows that these genes are most enriched in systemic lupus erythematosus ($P = 2.45 \times 10^{-5}$), Alcoholism ($P = 1.10 \times 10^{-4}$) and Neutrophil extracellular trap formation ($P = 1.20 \times 10^{-4}$); the gene ontology (GO) enrichment analysis shows the biological process (BP) of these pleiotropic genes is remarkably enriched in microtubule bundle formation ($P = 2.88 \times 10^{-4}$), axoneme assembly ($P = 1.86 \times 10^{-3}$) and regulation of mitotic cell cycle ($P = 1.95 \times 10^{-3}$). For the GO cellular component (CC) terms, these genes are concentrated in nucleosome ($P = 2.04 \times 10^{-4}$), neuron part ($P = 2.33 \times 10^{-3}$) and dendrite ($P = 4.36 \times 10^{-3}$). For the molecular function (MF) categories, these genes are enriched in structural constituent of chromatin ($P = 7.08 \times 10^{-4}$), protein kinase binding ($P = 4.27 \times 10^{-3}$) and acyltransferase activity ($P = 4.68 \times 10^{-3}$). However, the FDR adjusted p-values of
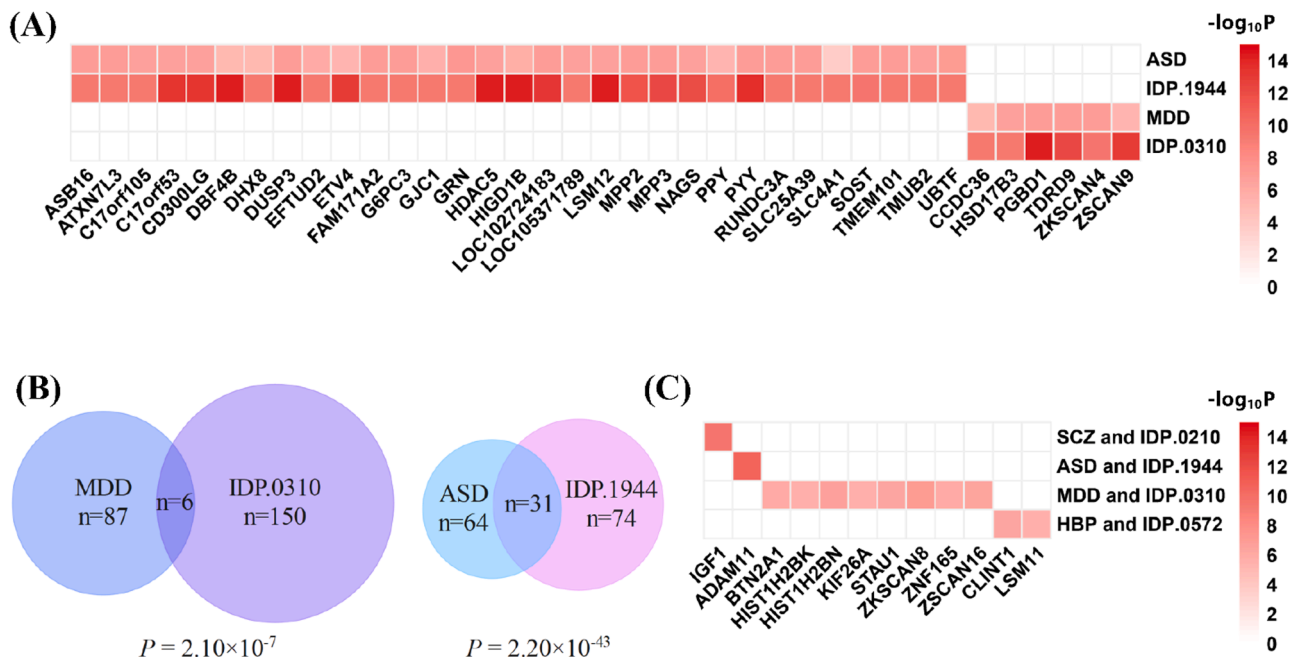

Fig. 6. Pleiotropic genes associated with the brain disorders/cardiovascular diseases and the brain IDPs discovered by MAGMA and PLACO. **A.** Genes ($FDR_{MAGMA} < 0.05$) simultaneously associated with both the IDP.1944 and ASD, and with both the brain IDP.0310 and MDD. Darker color indicates the higher significance evaluated by [$- log_{10}(P_{MAGMA})$]. **B.** Venn diagram to shown the number of shared genes ($FDR_{MAGMA} < 0.05$) between the between the brain IDP.1944 and ASD, and IDP.0310 and MDD. The P-value out the Venn diagram is the Fisher's exact test result showing the significance of shared genes between the IDPs and the diseases. **C.** The pleiotropic genes (Bonferroni corrected $P < 0.05$) identified by PLACO as associated with SCZ and IDP.0210, ASD and IDP.1944, MDD and IDP.0310, and hypertension (HBP) and IDP.0572 but not by MAGMA. Darker color indicates higher significance [$- log_{10}(P_{PLACO})$] of PLACO test on the gene associations between the IDPs and the disorders. IDP.0210: Volume of cerebellum-white-matter in the right hemisphere; IDP.1994: Mean ICVF in superior fronto-occipital fasciculus (right); IDP.0310: Volume of lateral posterior nucleus of thalamus in the left hemisphere; IDP.0572: Volume of superior temporal in the left hemisphere.

pathway enrichment are not significant at 0.05 threshold. By KOBAS, the KEGG enrichment analysis shows that these genes are most enriched in systemic lupus erythematosus ($P = 1.71 \times 10^{-5}$), Alcoholism ($P = 6.93 \times 10^{-5}$) and Viral carcinogenesis ($P = 1.29 \times 10^{-3}$). The gene ontology (GO) enrichment analysis shows the biological process (BP) of these pleiotropic genes is remarkably enriched in microtubule bundle formation ($P = 4.68 \times 10^{-4}$), G protein-coupled serotonin receptor signaling pathway ($P = 1.75 \times 10^{-3}$) and positive regulation of DNA-templated transcription ($P = 1.87 \times 10^{-3}$). For the GO cellular component (CC) terms, these genes are concentrated in nucleus ($P = 7.95 \times 10^{-5}$), nucleoplasm ($P = 5.21 \times 10^{-4}$) and plasma membrane ($P = 6.35 \times 10^{-4}$). For the molecular function (MF) categories, these genes are enriched in protein binding ($P = 3.70 \times 10^{-14}$), cAMP binding ($P = 1.50 \times 10^{-3}$) and hormone activity ($P = 1.64 \times 10^{-3}$). Only FDR adjusted p-values of protein binding ($P = 3.70 \times 10^{-14}$, $FDR = 1.73 \times 10^{-11}$) reaches the significant threshold ($FDR < 0.05$). We also performed PLACO analysis for all the brain IDPs and brain disorders/cardiovascular diseases. The results are shown in Supplementary Material.

4. Discussion

Observational studies have reported that IDPs are associated with various disorders; however, the precise nature of the genetic associations is still far from clear. In this study, we have investigated the genetic correlations and putatively causal relationships between 921 brain IDPs and 26 brain disorders and cardiovascular diseases by means of LDSC and MR analysis. We identified four brain IDPs with putatively causal effects on the neurological disorder, amyotrophic lateral sclerosis (ALS), and three psychiatric disorders, major depressive disorder (MDD), autism spectrum disorder (ASD) and schizophrenia (SCZ), suggesting the brain structure change causing these brain disorders. Moreover, we found putatively causal effects of hypertension on four IDPs, indicating the influence of hypertension on brain structures. Then, we utilized random skewed method to compare the $PCC_{dis\text{-}IDP\text{-}dis}$ (Pearson correlation coefficients (PCC) of $r_{gIDP\text{-}dis}$ for each pair of disorders/diseases) matrix with $r_{g\text{-}dis\text{-}dis}$ (genetic correlations between disorders/diseases) matrix. The results indicated that disorders/diseases sharing significant genetic associations tend to have similar genetic correlations with IDPs. Besides, although the MR analysis supports the casual relationships between brain IDPs and brain disorders/cardiovascular diseases, whether there are the genetic causal pathways shared between them is unknown. For such purpose, we used COLOC to test shared causal SNPs between brain IDPs and brain disorders/cardiovascular diseases, which have shown putative causal relationships in MR analysis. We further explored the shared genetic mechanisms potentially associated with both the brain disorders/cardiovascular diseases and the IDPs. Our analysis provides important new insights into the genetic background underlying these disorders at the imaging level.

Brain IDPs can be also considered as intermediate phenotypes to investigate the genetic correlations between various disorders. Intermediate phenotypes are traits positioned somewhere between genetic variation and disease, which represent a target for attempts to find disease-associated genetic variants and the shared mechanisms. In our study, we used brain IDPs as intermediate phenotypes to explore whether they can be a potential risk factor that may affect the outcome (i.e. brain disorders/cardiovascular diseases). We also used brain IDPs to discover candidate genes involved in the shared genetic mechanisms underlying brain disorders/cardiovascular diseases.

In this study, we identified putatively causal effects of four IDPs on psychiatric disorders, ASD, SCZ and MDD. The increase in the mean intracellular volume fraction (ICVF) value of the superior fronto-occipital fasciculus in the right hemisphere is likely to be a cause of ASD (IVW OR = 1.31, 95% CI of 1.17 to 1.46, $P = 1.49 \times 10^{-6}$). The fronto-occipital fasciculus is known to play a role in the control of neuropsychological behavior (D et al., 2021). And the increased ICVF appears to imply a reduction in the complexity of neurite density, which

supports the notion that ASD is associated with the loss of motor neurite density (DiPiero et al., 2023). A previous study has also observed higher fractional anisotropy in the superior fronto-occipital fasciculus of children with ASD than in controls (Cai et al., 2020). For SCZ, we identified the volume of cerebellar white matter in the right hemisphere as a putatively causal effect on this disorder (OR = 1.54, 95% CI 1.30–1.81, $P = 3.38 \times 10^{-7}$). Several previous studies have noted that an increased volume of cerebellar white-matter, possibly suggesting anomalous connectivity, is associated with SCZ (Lee et al., 2007; Kim et al., 2021; Klauser et al., 2017). This chimes with the observation that cerebellar white matter activity is a contributory factor to schizophrenia pathology (Yang et al., 2020; Papiol et al., 2014). Here, we provide genetic evidence to support these findings regarding the relationship between the IDPs and SCZ. The increase in the volume of the lateral posterior nucleus of thalamus (LP) in the left hemisphere is likely to be a cause of MDD (IVW OR = 1.22, 95% CI of 1.11 to 1.35, $P = 1.93 \times 10^{-5}$). The LP appears important for various functions including determining visual saliency, visually guided behaviors and multisensory processing of information related to aversive stimuli (Allen et al., 2016). Changes in the activity of these sites leads to abnormalities in the perception and interpretation of reward valence, in the motivation for behaviors, and in subsequent decision-making. Besides, the mean orientation dispersion index (ODI) in the right cerebral peduncle was identified as having a putatively causal effect on amyotrophic lateral sclerosis (ALS) (IVW OR = 0.80, 95% CI: 0.72 to 0.89, $P = 1.93 \times 10^{-5}$). The ODI is used to characterize the angular variation of neurites (Zhang et al., 2012a) and serves to reflect the severity of neurodegenerative disorders (Vogt et al., 2020; Zhang et al., 2012b). A reduced ODI appears to imply a reduction in the complexity of dendrites and axons (Zhang et al., 2012b). Consistent with our own results, previous studies have observed a significantly reduced ODI in ALS patients in the right internal capsule compared to controls (Broad et al., 2019; Kamagata et al., 2021).

The MR analysis indicated hypertension to be a likely causal effect on four IDPs, the volume and thickness of the superior segment of the temporal lobe in the right hemisphere, and the thickness of the middle temporal and inferior temporal lobe in the left hemisphere. A previous study showed that hypertension affects the structure of the inferior temporal lobe (Feng et al., 2020), suggesting that hypertension might be associated with reduced hippocampal connectivity and impaired memory. It has been noted that the volume and thickness of the inferior temporal lobe are significantly lower in hypertension patients than in controls (Sible et al., 2021) while another study has observed that the hypertension is associated with the structure of the middle temporal lobe (Sible and Nation, 2022). Here, we have provided genetic evidence for the causal effects of hypertension on the temporal lobe structure in both left and right hemispheres.

Fig. 4C summarized the brain structures associated the IDPs having causal relationships with the disorders. Briefly, the IDP associated with the right cerebral peduncle has a putatively causal effect on ALS. The IDP associated with the volume of lateral posterior (LP) nucleus of the thalamus, was found to have a putatively causal effect on MDD (Fig. 4C). Further, we identified the ICVF of the superior fronto-occipital fasciculus in the right hemisphere as a putatively causal effect on ASD. The IDP corresponding to the volume of right cerebellar white matter has a putatively causal effect on increased SCZ risk (Fig. 4C). Finally, hypertension was identified as having a putatively causal effect on the IDPs in the temporal lobe (superior, middle and inferior) (Fig. 4C), part of the brain which is associated with processing auditory information.

This study set out to investigate the genetic correlations between various disorders. As was to be expected, we found that the disorders from the same category exhibited stronger genetic correlations than the disorders from different categories. Interestingly, we found that stroke was genetically correlated with all the cardiovascular diseases (CA, AP, HBP, MI, CH and HF) investigated in this study (Supplementary Figure 3A). Moreover, the genetic correlations ($r_{gIDP\text{-}STR}$) between stroke and the IDPs were also significantly correlated with $r_{gIDP\text{-}dis}$ between the

cardiovascular diseases and the IDPs (Fig. 3A), suggesting that the IDP measures for the cardiovascular diseases may also have the potential to characterize stroke.

We also found that stroke was genetically correlated with the psychiatric disorders, PTSD, ADHD and MDD (Supplementary Figure 3). A 9-year follow up study has previously indicated that patients with MDD have an increased tendency to experience stroke as compared to the general population without MDD (Li et al., 2012). Other studies have indicated that stroke survivors display an increased risk of developing depression or other mood disorders compared to the general population (Skajaa et al., 2022; Allan et al., 2013). For example, the most recent study of 86,111 stroke survivors showed that they had a 15% risk of developing a mood disorder, primarily depression, which is significantly higher than the general population (Skajaa et al., 2022). Clinical studies have also noted a significant correlation between stroke and ADHD: one study followed up 13,141 samples with childhood stroke and matched controls, and found a 2-fold increased risk of ADHD after stroke (Bolk et al., 2022). Clinically, PTSD has long been recognized as a risk factor for stroke (Kronish et al., 2014; Perkins et al., 2021). Here, we have presented genetic evidence that may help us to interpret the relationship between stroke and the psychiatric disorders, as well as providing the IDPs that may serve as preclinical indicators of the risk of stroke and/or psychiatric disorders. These findings are therefore potentially important for the early diagnosis or prevention of both stroke and psychiatric disorders.

We also carried out gene-based pleiotropy analysis for the various disorders/diseases and IDPs. Compared to previous studies that mainly focused on identifying pleiotropic associations between disorders, our work has two pronounced advantages. First, we have shown that those disorders that share significant genetic associations also tend to share significant genetic associations with the same IDPs. Second, we explain the genetic correlations between two disorders from the perspective of brain morphology by applying PLACO to detect genes with pleiotropic effects between any two disorders and their co-associated IDPs. This investigation was designed under the assumption that one phenotype can share similar genetic components with the others under the influence of pleiotropic genes (Lu et al., 2021). We found that the genes associated with MDD, AN, BID and ADHD also tended to be associated with the IDPs associated with corona radiata, capsule and corpus callosum (Supplementary Figure 5A and Supplementary Figure 6C). Additionally, the genes associated with hypertension, MI, HF and CA were also found to be associated with the IDPs in the thalamus and corona radiata (Supplementary Figure 5C and Supplementary Figure 6D).

The gene-based PLAOC test further identified many genes simultaneously associated with IDPs from multiple brain regions and also with the cardiovascular diseases or the brain disorders. For example, genes, *ZSCAN9, PGBD1* and *ZKSCAN4* were pleiotropic genes for MDD, AN, BID, ADHD and brain IDPs from corona radiata, capsule and corpus callosum; *TMEM116, ERP29* and *MAPKAPK5* were found as pleiotropic genes of HBP, MI, HF and CA, and brain IDPs from thalamus and corona radiata (Supplementary Figure 6C-D and Supplementary Figure 7). The *ZSCAN9* gene encodes a transcription factor that has been suggested to be associated with the MDD, BID and SCZ in a previous cohort study (Raskó et al., 2022). The *PGBD1* gene is known to be involved in the core functionality of the brain (Yue et al., 2011), and mutations within *PGBD1* may be associated with psychiatric disorders (Raskó et al., 2022). In addition, the *ZKSCAN4* gene has been identified as one of the most compelling risk genes associated with broad phenotypes related to psychosis (Yue et al., 2011; Sun et al., 2015a). Interestingly, *PGBD1* gene is a paralog of *ZSCAN12*. Thus, all three genes may be part of the same Zinc finger protein family, and their variants could be involved in regulating the expression of psychosis-related genes, especially those genes involving the dopamine pathway (Sun et al., 2015b). *TMEM116* encodes a transmembrane protein which plays a role in blood coagulation (Yang et al., 2012) and has been suggested as the potential CA gene

in a previous study (Brænne et al., 2015). The *ERP29* gene, which is thought to play a role in the processing of secretory proteins in the ER, may be involved in the development of ischemic heart disease (Azfer et al., 2006). Loss-of-function variants in *MAPKAPK5* are known to cause neurocardiofaciodigital (NCFD) syndrome which is characterized by malformations of the heart and severe neurodevelopmental disturbances (Horn et al., 2021). This is the first time all these genes are reported as associated with brain IDPs, brain disorders, and cardiovascular diseases.

This study has several limitations. First, the sample sizes of GWAS summary statistics of many disorders may be insufficient, thereby limiting the power of this study to identify putative causal relationships between the various disorders and the IDPs. Second, some disorders such as MDD, BID and ASD have insufficient (<10) instrumental SNPs ($P < 5 \times 10^{-8}$) to allow testing with MR models. Thus, additional GWAS studies of these disorders will be required for us to detect associations with IDPs. Third, the GWAS of IDPs were generated from samples derived from the UK-Biobank. Although we avoided using the GWAS summary statistics of the disorders based on samples in the UK-Biobank, we were unable to estimate the percentages of the sample overlap between the IDPs and the disorders because we did not have the sample information. Besides, multiple-source genomic data can be integrated into our study to reveal the specific mechanisms of brain disorders (Horn et al., 2021).

In conclusion, this study performed bidirectional two-sample MR analyses to systematically estimate the underlying causal relationships between brain imaging-derived phenotypes (IDPs) and the risk of brain disorders and/or cardiovascular diseases using large-scale GWAS data. Our analysis revealed strong genetic evidence for causal relationships between IDPs and various disorders, which has the potential to contribute to early diagnosis of brain and cardiovascular diseases through brain-imaging biomarkers. Additionally, this study identified many pleiotropic genes that are significantly associated with these disorders and IDPs, which could reflect the shared genetic mechanisms involving brain structural changes and the occurrence of the brain disorders and cardiovascular diseases.

Data and code availability statement

UK Biobank data are available through an application process. GWAS data are openly available from the Psychiatric Genomics Consortium (PGC) at https://pgc.unc.edu/ and NHGRI-EBI GWAS Catalog data at https://www.ebi.ac.uk/gwas/. All data generated or analyzed during this study are included in this published article and its supplementary information files.

The Linkage disequilibrium score regression (LDSC) analysis was performed by third party code at https://github.com/bulik/ldsc (version 1.0.1). The Mendelian randomization (MR) analyses were performed by R packages TwoSampleMR (version 0.5.5) and GSMR (version 1.0.9). The colocalization analysis was performed by R packages COLOC (version 5). The MAGMA analysis was performed by third party code at https://ctg.cncr.nl/software/magma. The PLACO analysis was performed by third party code at https://github.com/RayDebashree/PLACO.

Ethics statement

Informed consent was obtained from all UK Biobank participants. Ethical procedures are controlled by a dedicated Ethics Advisory Committee (http://www.ukbiobank.ac.uk/ethics).

Declaration of Competing Interest

The authors declare that they have no known competing financial interests or personal relationships that could have appeared to influence the work reported in this paper.

Data availability

Data will be made available on request.

Acknowledgements

We'd like to thank the UK Biobank (application number #51732) and FinnGen project to make the data available.

Supplementary materials

Supplementary material associated with this article can be found, in the online version, at doi:10.1016/j.neuroimage.2023.120325.

References

Allan, L.M., Rowan, E.N., Thomas, A.J., Polvikoski, T.M., O'Brien, J.T., Kalaria, R.N., 2013. Long-term incidence of depression and predictors of depressive symptoms in older stroke survivors. Br. J. Psychiatry 203 (6), 453–460.

Allen, A.E., Procyk, C.A., Howarth, M., Walmsley, L., Brown, T.M., 2016. Visual input to the mouse lateral posterior and posterior thalamic nuclei: photoreceptive origins and retinotopic order. J. Physiol. (Lond.) 594 (7), 1911–1929.

Azfer, A., Niu, J., Rogers, L.M., Adamski, F.M., Kolattukudy, P.E., 2006. Activation of endoplasmic reticulum stress response during the development of ischemic heart disease. Am. J. Physiol.-Heart Circulat. Physiol. 291 (3), H1411–H1420.

Boedhoe, P.S., et al., 2020. Subcortical brain volume, regional cortical thickness, and cortical surface area across disorders: findings from the ENIGMA ADHD, ASD, and OCD working groups. Am. J. Psychiatry 177 (9), 834–843.

Bolk, J., Simatou, E., Soderling, J., Thorell, L.B., Persson, M., Sundelin, H., 2022. Association of Perinatal and Childhood Ischemic Stroke With Attention-Deficit/Hyperactivity Disorder. JAMA Netw. Open 5 (4), e228884.

Bowden, J., Smith, G.Davey, Burgess, S., 2015. Mendelian randomization with invalid instruments: effect estimation and bias detection through Egger regression. Int. J. Epidemiol. 44 (2), 512–525.

Bowden, J., Smith, G.Davey, Haycock, P.C., Burgess, S., 2016. Consistent estimation in Mendelian randomization with some invalid instruments using a weighted median estimator. Genet. Epidemiol. 40 (4), 304–314.

Brænne, I., et al., 2015. Prediction of causal candidate genes in coronary artery disease loci. Arterioscler. Thromb. Vasc. Biol. 35 (10), 2207–2217.

Broad, R.J., et al., 2019. Neurite orientation and dispersion density imaging (NODDI) detects cortical and corticospinal tract degeneration in ALS. J. Neurol. Neurosurg. Psychiatry 90 (4), 404–411.

Bulik-Sullivan, B.K., et al., 2015a. LD Score regression distinguishes confounding from polygenicity in genome-wide association studies. Nat. Genet. 47 (3), 291–295.

Bulik-Sullivan, B., et al., 2015b. An atlas of genetic correlations across human diseases and traits. Nat. Genet. 47 (11), 1236–1241.

Burgess, S., Dudbridge, F., Thompson, S.G., 2016. Combining information on multiple instrumental variables in Mendelian randomization: comparison of allele score and summarized data methods. Stat. Med. 35 (11), 1880–1906.

Cai, K., et al., 2020. Mini-Basketball Training Program Improves Social Communication and White Matter Integrity in Children with Autism. Brain Sci. 10 (11).

Cheverud, J.M., 1996. Quantitative genetic analysis of cranial morphology in the cotton-top (Saguinus oedipus) and saddle-back (S. fuscicollis) tamarins. J. Evol. Biol. 9 (1), 5–42.

D, E.B.A, Marras, C.E., Petit, L., Sarubbo, S., 2021. The inferior fronto-occipital fascicle: a century of controversies from anatomy theaters to operative neurosurgery. J. Neurosurg. Sci. 65 (6), 605–615.

de Leeuw, C.A., Mooij, J.M., Heskes, T., Posthuma, D., 2015. MAGMA: generalized gene-set analysis of GWAS data. PLoS Comput. Biol. 11 (4), e1004219.

DiPiero, M.A., Surgent, O.J., Travers, B.G., Alexander, A.L., Lainhart, J.E., Dean III, D.C., 2023. Gray matter microstructure differences in autistic males: a gray matter based spatial statistics study. NeuroImage: Clinical 37, p. 103306.

Elliott, L.T., et al., 2018. Genome-wide association studies of brain imaging phenotypes in UK Biobank. Nature 562 (7726), 210–216.

Emdin, C.A., Khera, A.V., Kathiresan, S., 2017. Mendelian randomization. JAMA 318 (19), 1925–1926.

Feng, R., Rolls, E.T., Cheng, W., Feng, J., 2020. Hypertension is associated with reduced hippocampal connectivity and impaired memory. EBioMedicine 61, 103082.

Foley, C.N., et al., 2021. A fast and efficient colocalization algorithm for identifying shared genetic risk factors across multiple traits. Nat. Commun. 12 (1), 764.

Giambartolomei, C., et al., 2014a. Bayesian test for colocalisation between pairs of genetic association studies using summary statistics. PLoS Genet. 10 (5), e1004383.

Giambartolomei, C., et al., 2014b. Bayesian test for colocalisation between pairs of genetic association studies using summary statistics. PLoS Genet. 10 (5), e1004383.

Giambartolomei, C., et al., 2018. A Bayesian framework for multiple trait colocalization from summary association statistics. Bioinformatics 34 (15), 2538–2545.

Gong, W., Beckmann, C.F., Smith, S.M., 2021. Phenotype discovery from population brain imaging. Med. Image Anal. 71, 102050.

Guo, J., et al., 2022. Mendelian randomization analyses support causal relationships between brain imaging-derived phenotypes and risk of psychiatric disorders. Nat. Neurosci. 25 (11), 1519–1527.

Gurillo, P., Jauhar, S., Murray, R.M., MacCabe, J.H., 2015. Does tobacco use cause psychosis? Systematic review and meta-analysis. The Lancet Psychiatry 2 (8), 718–725.

Hajjar, I., et al., 2011. Hypertension, white matter hyperintensities, and concurrent impairments in mobility, cognition, and mood: the Cardiovascular Health Study. Circulation 123 (8), 858–865.

Hartwig, F.P., Smith, G.Davey, Bowden, J., 2017. Robust inference in summary data Mendelian randomization via the zero modal pleiotropy assumption. Int. J. Epidemiol. 46 (6), 1985–1998.

Horn, D., et al., 2021. Biallelic truncating variants in MAPKAPK5 cause a new developmental disorder involving neurological, cardiac, and facial anomalies combined with synpolydactyly. Genet. Med. 23 (4), 679–688.

Kamagata, K., et al., 2021. Diffusion Magnetic Resonance Imaging-Based Biomarkers for Neurodegenerative Diseases. Int. J. Mol. Sci. 22 (10).

Kim, S.E., Jung, S., Sung, G., Bang, M., Lee, S.H., 2021. Impaired cerebro-cerebellar white matter connectivity and its associations with cognitive function in patients with schizophrenia. NPJ Schizophr. 7 (1), 38.

Klauser, P., et al., 2017. White Matter Disruptions in Schizophrenia Are Spatially Widespread and Topologically Converge on Brain Network Hubs. Schizophr. Bull. 43 (2), 425–435.

Knutson, K.A., Pan, W., 2020. Integrating brain imaging endophenotypes with GWAS for Alzheimer's disease. Quant. Biol. 1–16.

Kronish, I.M., Lin, J.J., Cohen, B.E., Voils, C.I., Edmondson, D., 2014. Posttraumatic stress disorder and medication nonadherence in patients with uncontrolled hypertension. JAMA Intern. Med. 174 (3), 468–470.

Lee, K.H., et al., 2007. Increased cerebellar vermis white-matter volume in men with schizophrenia. J. Psychiatr. Res. 41 (8), 645–651.

Li, C.T., et al., 2012. Major depressive disorder and stroke risks: a 9-year follow-up population-based, matched cohort study. PLoS ONE 7 (10), e46818.

Li, L., et al., 2021. Lower regional grey matter in alcohol use disorders: evidence from a voxel-based meta-analysis. BMC Psychiatry 21 (1), 1–11.

Liang, Y., Melia, O., Caroll, T.J., Brettin, T., Brown, A., Im, H.K., 2022. BrainXcan identifies brain features associated with behavioral and psychiatric traits using large scale genomic and imaging data. medRxiv, p. 2021.06. 01.21258159.

Lu, H., Qiao, J., Shao, Z., Wang, T., Huang, S., Zeng, P., 2021. A comprehensive gene-centric pleiotropic association analysis for 14 psychiatric disorders with GWAS summary statistics. BMC Med. 19 (1), 1–17.

MacArthur, J., et al., 2017. The new NHGRI-EBI Catalog of published genome-wide association studies (GWAS Catalog). Nucleic Acids Res. 45 (D1), D896–D901.

May-Wilson, S., et al., 2022. Large-scale GWAS of food liking reveals genetic determinants and genetic correlations with distinct neurophysiological traits. Nat. Commun. 13 (1), 2743.

McCracken, C., et al., 2022. Multi-organ imaging demonstrates the heart-brain-liver axis in UK Biobank participants. Nat. Commun. 13 (1), 7839.

Miller, K.L., et al., 2016. Multimodal population brain imaging in the UK Biobank prospective epidemiological study. Nat. Neurosci. 19 (11), 1523–1536.

Noble, K.G., et al., 2015. Family income, parental education and brain structure in children and adolescents. Nat. Neurosci. 18 (5), 773–778.

Papiol, S., et al., 2014. Polygenic determinants of white matter volume derived from GWAS lack reproducibility in a replicate sample. Transl. Psychiatry 4 (2) e362-e362.

Perkins, J.D., Wilkins, S.S., Kamran, S., Shuaib, A., 2021. Post-traumatic stress disorder and its association with stroke and stroke risk factors: a literature review. Neurobiol. Stress 14, 100332.

Purcell, S., et al., 2007. PLINK: a tool set for whole-genome association and population-based linkage analyses. Am. J. Hum. Gen. 81 (3), 559–575.

Raskó, T., et al., 2022. A novel gene controls a new structure: piggyBac Transposable Element-derived 1, unique to mammals, controls mammal-specific neuronal paraspeckles. Mol. Biol. Evol. 39 (10), p. msac175.

Ray, D., Chatterjee, N., 2020. A powerful method for pleiotropic analysis under composite null hypothesis identifies novel shared loci between Type 2 Diabetes and Prostate Cancer. PLoS Genet. 16 (12), e1009218.

Revell, L.J., 2012. phytools: an R package for phylogenetic comparative biology (and other things). Methods Ecol. Evol. (2), 217–223.

Rohlf, F.J., 2017. The method of random skewers. Evol. Biol. 44 (4), 542–550.

Sarıçiçek, A., 2016. Abnormal white matter integrity as a structural endophenotype for bipolar disorder. Psychol. Med. 46 (7), 1547–1558.

Schneider, C.E., et al., 2014. Smoking status as a potential confounder in the study of brain structure in schizophrenia. J. Psychiatr. Res. 50, 84–91.

Sible, I.J., Nation, D.A., I. Alzheimer's Disease Neuroimaging, 2022. Visit-to-Visit Blood Pressure Variability and Longitudinal Tau Accumulation in Older Adults. Hypertension 79 (3), 629–637.

Sible, I.J., et al., 2021. Visit-to-visit blood pressure variability and regional cerebral perfusion decline in older adults. Neurobiol. Aging 105, 57–63.

Skajaa, N., et al., 2022. Stroke and Risk of Mental Disorders Compared With Matched General Population and Myocardial Infarction Comparators. Stroke 53 (7), 2287–2298.

Smith, S.M., et al., 2021. An expanded set of genome-wide association studies of brain imaging phenotypes in UK Biobank. Nat. Neurosci. 24 (5), 737–745.

Sun, Y., et al., 2015a. Association between variants of zinc finger genes and psychiatric disorders: systematic review and meta-analysis. Schizophr. Res. 162 (1–3), 124–137.

Sun, Y., et al., 2015b. Association between variants of zinc finger genes and psychiatric disorders: systematic review and meta-analysis. Schizophr. Res. 162 (1–3), 124–137.

Verbanck, M., Chen, C.Y., Neale, B., Do, R., 2018. Detection of widespread horizontal pleiotropy in causal relationships inferred from Mendelian randomization between complex traits and diseases. Nat. Genet. 50 (5), 693–698.

Vogt, N.M., et al., 2020. Cortical Microstructural Alterations in Mild Cognitive Impairment and Alzheimer's Disease Dementia. Cereb. Cortex 30 (5), 2948–2960.

Vreeker, A., et al., 2021. Genetic analysis of activity, brain and behavioral associations in extended families with heavy genetic loading for bipolar disorder. Psychol. Med. 51 (3), 494–502.

Wei, Y., Bresser, T., Wassing, R., Stoffers, D., Van Someren, E.J.W., Foster-Dingley, J.C., 2019. Brain structural connectivity network alterations in insomnia disorder reveal a central role of the right angular gyrus. Neuroimage Clin. 24, 102019.

Xie, C., et al., 2011. KOBAS 2.0: a web server for annotation and identification of enriched pathways and diseases. Nucleic Acids Res. 39 (suppl_2), W316–W322.

Yang, H., et al., 2012. TMEM16F forms a Ca2+-activated cation channel required for lipid scrambling in platelets during blood coagulation. Cell 151 (1), 111–122.

Yang, M., Gao, S., Zhang, X., 2020. Cognitive deficits and white matter abnormalities in never-treated first-episode schizophrenia. Transl. Psychiatry 10 (1), 1–8.

Yue, W.H., et al., 2011. Genome-wide association study identifies a susceptibility locus for schizophrenia in Han Chinese at 11p11.2. Nat. Genet. 43 (12), 1228–1231.

Zhang, H., Schneider, T., Wheeler-Kingshott, C.A., Alexander, D.C., 2012a. NODDI: practical in vivo neurite orientation dispersion and density imaging of the human brain. Neuroimage 61 (4), 1000–1016.

Zhang, H., Schneider, T., Wheeler-Kingshott, C.A., Alexander, D.C., 2012b. NODDI: practical in vivo neurite orientation dispersion and density imaging of the human brain. Neuroimage 61 (4), 1000–1016.

Zhao, B., et al., 2021. Common genetic variation influencing human white matter microstructure. Science 372 (6548), eabf3736.

Zhou, Y., et al., 2019. Metascape provides a biologist-oriented resource for the analysis of systems-level datasets. Nat. Commun. 10 (1), 1523.

Zhu, Z., et al., 2018. Causal associations between risk factors and common diseases inferred from GWAS summary data. Nat. Commun. 9 (1), 1–12.